New Boundary Integral Equations for CAD of Waveguide Circuits: Guided-Mode Extracted Integral Equations

Kazuo Tanaka *Member, IEEE,* and Masaaki Nakahara

***Abstract*—Novel boundary integral equations which are applicable to the analysis of many kinds of waveguide circuits are presented. The new integral equations can treat the waveguide discontinuity problems like the scattering by the isolated finite-sized metallic objects or cavity problems and do not employ normal-mode expansion techniques. They are suitable for the basic theory of CAD software for various waveguide circuits. The 2-port and H-plane waveguide discontinuity problems which satisfy the single-mode and two-mode conditions are treated in this paper. The case of waveguide corner bend is considered as an example. The numerical examples are shown in order to confirm the validity of the new integral equations.**

I. Introduction

WITH the development of computer-aided design (CAD) of complicated waveguide circuits or discontinuities, numerical approaches such as boundary element method (moment method) based on integral equation methods occupy attentions of many researchers. References [1]–[6]. In the direct application of these integral equation methods to waveguide discontinuity problems, we often encounter the treatment of integral along infinite region of the uniform waveguide. In order to avoid this difficulty, various techniques based on normal-mode expansion theory are often employed in the integral equation methods. However, these methods based on the normal-mode expansion techniques will be very complicated in the application of CAD software for the various three-dimensional waveguide circuits or open dielectric waveguide circuits of complicated configuration.

In this paper, novel boundary integral equations which are applicable to the analysis of many kinds of waveguide circuits are presented [7]. Since new integral equations can treat the waveguide discontinuity problems like the scattering by the isolated finite-sized metallic objects or cavity problems and do not employ the normal-mode expansion techniques, they are very suitable for the basic theory of CAD software for various waveguide circuits. The 2-port waveguide discontinuity problems are considered. The case of waveguide corner bend is considered in this paper. Considering rather simple problems, we can show the basic idea and discovery which are used in deriving new integral equations. We treat the case of H-plane waveguide discontinuity problems which satisfy the single-mode and two-mode conditions. The numerical examples of the 2-port waveguide circuits are shown in order to confirm the validity of the new integral equations.

Manuscript received June 25, 1991; revised January 8, 1992. This work was supported in part by funding from The Okawa Institute of Information and Telecommunication in Japan.

The authors are with the Department of Electronics and Computer Engineering, Gifu University, Gifu City, Yanagido 1-1, Japan 501-11.

IEEE Log Number 9200851.

II. Waveguide Bends

Since the new boundary integral equations for the general waveguide circuit have complicated expressions, we restrict our attention to a simple two-ports circuit, i.e., the arbitrary-shaped waveguide bend as shown in Fig. 1. For the mathematical simplicity, we consider the H-plane waveguide discontinuity problem. The time factor exp $(j\omega t)$ is understood. The waveguide 1 of width $2k_0a_1$ and waveguide 2 of width $2k_0a_2$ are joined together to form angle θ_2-θ_1 through the connection section of arbitrary-shape as shown in Fig. 1, where wavenumber k_0 is given by $k_0 = \omega/c$ and c is light velocity in vacuum. It is assumed that both waveguides are filled with dielectric of relative permittivity ϵ_r. We first consider the case where they satisfy the single-mode condition. We denote the boundaries of both waveguides by C_1, C_2, C_3 and C_4, and those of the connection section by C_5 and C_6. We also denote the virtual boundaries between two waveguides and the connection section by C_{10} and C_{20} as shown in Fig. 1. A TE_{10} mode denoted by $E^{-(2)}(x)$ is incident from the waveguide 2 to the connection section. We denote the z component of the total electric field by $E(x)$. From Maxwell's equations and Green's theorem, the conventional boundary integral representation for the total field $E(x)$ is written as

$$E(x) = \int_C G(x|x')\, \partial E(x')/\partial n'\, dl' \tag{1}$$

where

$$G(x|x') = -j/4 H_0^{(2)}(n_r k_0 |x - x'|), \tag{2}$$

$C = C_1 + C_2 + C_3 + C_4 + C_5 + C_6$, $n_r = (\epsilon_r)^{1/2}$, $\partial/\partial n$ represents the derivatives normal to C_1–C_6, in the outward direction and vector $x = (x, y) = (r, \theta)$ and $x' = (x', y')$ denote the observation point and source point, respectively, in the coordinate system shown in Fig. 1. The in-

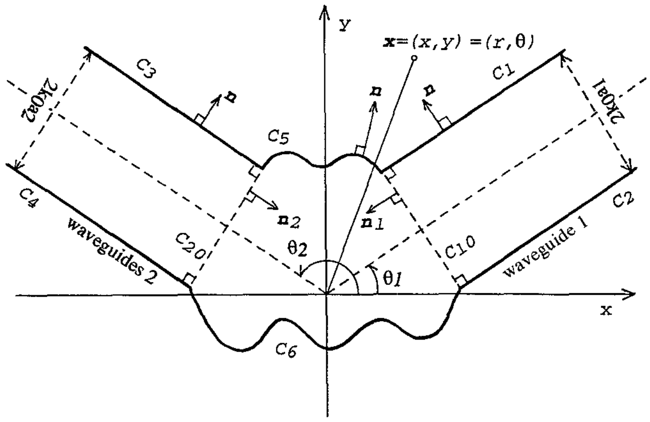

Fig. 1. Waveguide bend with arbitrary shaped connection section.

cident wave is reflected and transmitted by the bend. The reflected wave in the waveguide 2 and transmitted wave in the waveguide 1 are denoted by $S_{22}E^{+(2)}(x)$ and $S_{21}E^{+(1)}(x)$, respectively, where S_{22} and S_{21} are reflection and transmission coefficients, respectively. The coefficients S_{21} and S_{22} are referred to the section C_{10} and C_{20}, respectively, shown in Fig. 1. The total field $E(x)$ will be very complicated in the vicinity of the connection section. Only the reflected wave plus the incident wave, however, can survive at points far away from the bend in the waveguide 2 and only the transmitted wave can survive at points far away in the waveguide 1, So, we decompose the total field $E(x)$ in the waveguides 1 and 2 into field components as

$$E(x) = E^C(x) + S_{21}E^{+(1)}(x), \qquad \text{in the waveguide 1,} \tag{3}$$

$$E(x) = E^C(x) + S_{22}E^{+(2)}(x) + E^{-(2)}(x), \qquad \text{in the waveguide 2,} \tag{4}$$

respectively. The field denoted by $E^C(x)$ is the difference between the total field and the transmitted wave in the waveguide 1 and the difference between the total field and the reflected and incident waves in the waveguide 2. The field $E^C(x)$ is called the disturbed field in this paper [7]–[10]. For convenience of notation we denote the total field in the connection section by the same symbol E^C used for the disturbed field in the waveguieds:

$$E(x) = E^C(x) \qquad \text{in the connection section.} \tag{5}$$

We first consider the case where the observation point x is placed at a point far away from the connection section in the waveguide 1. Substituting (3) and (4) into (1), we can obtain the following equation:

$$E^C(x) + S_{21}\left[E^{+(1)}(x) - \int_{C_1+C_2} G(x|x')\, \partial E^{+(1)}(x')/\partial n'\, dl'\right]$$
$$= \int_C G(x|x')\, \partial E^C(x')/\partial n'\, dl' + S_{22}\int_{C_3+C_4} G(x|x')\, \partial E^{+(2)}(x')/\partial n'\, dl' + \int_{C_3+C_4} G(x|x')\, \partial E^{-(2)}(x')/\partial n'\, dl'. \tag{6}$$

The semi-infinite line integrals of the mode functions $E^{+(1)}(x)$ and $E^{\pm(2)}(x)$ along $C_1 + C_2$ and $C_3 + C_4$ can be substituted by line integral along virtual boundary C_{10} and C_{20} by using Green's theorem. We have:

$$E^{+(1)}(x) - \int_{C_1+C_2} G(x|x')\, \partial E^{+(1)}(x')/\partial n'\, dl' = U^{+(1)}(x) \qquad (x \text{ to the right of } C_{10})$$
$$- \int_{C_1+C_2} G(x|x')\, \partial E^{+(1)}(x')/\partial n'\, dl' = U^{+(1)}(x) \qquad (x \text{ to the left of } C_{10}) \tag{7}$$

where

$$U^{+(1)}(x) = \int_{C_{10}} [G(x|x')\, \partial E^{+(1)}(x')/\partial n_1' - E^{+(1)}(x')\, \partial G(x|x')/\partial n_1']\, dl' \tag{8}$$

and

$$E^{\pm(2)}(x) - \int_{C_3+C_4} G(x|x')\, \partial E^{\pm(2)}(x')/\partial n'\, dl' = U^{\pm(2)}(x) \qquad (x \text{ to the left of } C_{20}),$$
$$- \int_{C_3+C_4} G(x|x')\, \partial E^{\pm(2)}(x')/\partial n'\, dl' = U^{\pm(2)}(x) \qquad (x \text{ to the right of } C_{20}) \tag{9}$$

where

$$U^{\pm(2)}(x) = \int_{C_{20}} [G(x|x')\, \partial E^{\pm(2)}(x')/\partial n_2' - E^{\pm(2)}(x')\, \partial G(x|x')/\partial n_2']\, dl' \tag{10}$$

respectively, and the unit vector n_j ($j = 1, 2$) normal to virtual boundaries C_{j0} ($j = 1, 2$) are shown in Fig. 1. By using (7) and (9), we can rewrite (6) as

$$E^C(x) + S_{21}U^{\pm(1)}(x) = \int_C G(x|x')\, \partial E^C(x')/\partial n'\, dl' - S_{22}U^{+(2)}(x) - U^{-(2)}(x). \qquad (x \text{ to the right of } C_{10}) \tag{11}$$

Since we can put the observation point x in (11) at a point far away ($r \to \infty$, $\theta = \theta_1$) from the connection section in the waveguide 1, we can use the asymptotic expansion of Green's function in (11) as

$$G(x|x') = G(r, \theta|x') = A(r)g(\theta|x') + o[(k_0r)^{-3/2}], \tag{12}$$

where

$$A(r) = -j/4\,[2j/(\pi n_r k_0 r)]^{1/2} \exp(-jn_r k_0 r) \quad (13)$$

$$g(\theta|x') = \exp(jn_r k_0 x' \cos\theta + jn_r k_0 y' \sin\theta). \quad (14)$$

Since the metallic waveguide cannot support waves of the form $A(r)$ along its boundary, the following conditions must be held:

$$\lim_{r\to\infty} E^C(r, \theta_1)/A(r) = 0,$$
$$\lim_{r\to\infty} E^C(r, \theta_2)/A(r) = 0. \quad (15)$$

We substitute asymptotic expression (12) into (11), divide both sides of the resulting equation by the common function $A(r)$ and set $\theta = \theta_1$ and $r \to \infty$ in the final equation. If we use the conditions (15), we can obtain the following equation:

$$S_{21}M^{+(1)}(\theta_1) + S_{22}M^{+(2)}(\theta_1) = \int_C g(\theta_1|x')\,\partial E^C(x')/\partial n'\,dl' - M^{-(2)}(\theta_1) \quad (16)$$

where

$$M^{\pm(j)}(\theta) = \int_{C_{j0}} [\,g(\theta|x')\,\partial E^{\pm(j)}(x')/\partial n_j' - E^{\pm(j)}(x') \cdot \partial g(\theta|x')/\partial n_j'\,]\,dl' \quad (j = 1, 2) \quad (17)$$

We next consider a condition that must hold at a point far away from the connection section in the waveguide 2. By the same procedure as that used in deriving (16), we can obtain the following equation:

$$S_{21}M^{+(1)}(\theta_2) + S_{22}M^{+(2)}(\theta_2) = \int_C g(\theta_2|x')\,\partial E^C(x')/\partial n'\,dl' - M^{-(2)}(\theta_2). \quad (18)$$

If we solve (16) and (18) for unknown constants S_{21} and S_{22}, then they can be expressed in terms of the disturbed field $\partial E^C(x)/\partial n$ on the walls of the two waveguides and of the total field $\partial E^C(x)/\partial n = \partial E(x)/\partial n$ on the wall of the connection section as

$$S_{21} = \left[\int_C W(x')\,\partial E^C(x')/\partial n'\,dl' + M^{-(2)}(\theta_2)M^{+(2)}(\theta_1) - M^{-(2)}(\theta_1)M^{+(2)}(\theta_2)\right]\Big/\Delta \quad (19)$$

$$S_{22} = \left[\int_C V(x')\,\partial E^C(x')/\partial n'\,dl' + M^{-(2)}(\theta_1)M^{+(1)}(\theta_2) - M^{-(2)}(\theta_2)M^{+(1)}(\theta_1)\right]\Big/\Delta \quad (20)$$

where

$$W(x') = M^{+(2)}(\theta_2)g(\theta_1|x') - M^{+(2)}(\theta_1)g(\theta_2|x') \quad (21)$$

$$V(x') = M^{+(1)}(\theta_1)g(\theta_2|x') - M^{+(1)}(\theta_2)g(\theta_1|x') \quad (22)$$

$$\Delta = M^{+(1)}(\theta_1)M^{+(2)}(\theta_2) - M^{+(2)}(\theta_1)M^{+(1)}(\theta_2). \quad (23)$$

III. New Boundary Integral Equation

Since the reflection and transmission coefficients can be expressed in terms of the field $\partial E^C(x)/\partial n$, the conventional integral representation (1) can be rewritten in terms of only the field $E^C(x)$ by substituting (3), (4), (5), (19) and (20) into (1) as

$$E^C(x) = \int_C P(x|x')\,\partial E^C(x')/\partial n'\,dl' + F^i(x) \quad (24)$$

where

$$P(x|x') = G(x|x') - [U^{+(1)}(x)W(x') + U^{+(2)}(x)V(x')]/\Delta \quad (25)$$

$$\begin{aligned}F^i(x) = &- U^{-(2)}(x)\\ &- U^{+(1)}(x)[M^{+(2)}(\theta_1)M^{-(2)}(\theta_2) - M^{+(2)}(\theta_2)M^{-(2)}(\theta_1)]/\Delta\\ &- U^{+(2)}(x)[M^{-(2)}(\theta_1)M^{+(1)}(\theta_2) - M^{-(2)}(\theta_2)M^{+(1)}(\theta_1)]/\Delta.\end{aligned} \quad (26)$$

If we introduce the boundary condition that the total and disturbed electric fields must vanish on the boundaries $C = C_1 + C_2 + C_3 + C_4 + C_5 + C_6$, we can obtain the new integral equation as follows:

$$0 = \int_C P(x|x')\,\partial E^C(x')/\partial n'\,dl' + F^i(x) \quad (27)$$

The integral equation (27) is compared with the conventional equation obtained by introducing the boundary condition to (1) in Table I. We find that the integral equation (27) also extends over the same infinite region C as in the conventional integral equation. However, the disturbed field become zero in the region sufficiently far away from the connection section, so that, in equation (27), C can be considered a finite region. So, we can perform the numerical analysis of (27) directly. Apart from the difference in the kernel and in the impresses function, we find that the basic structure of (27) is same as that of the conventional one. So, we can apply various techniques that were developed for solving the conventional equation to solve the boundary integral equation (27). Since we can consider that, in the kernel function $P(x|x')$, the part depending on the guided mode is extracted from the conventional kernel function $G(x|x')$, we can call this type of integral equation the guided-mode extracted integral equation (GMEIE).

TABLE I
COMPARISON BETWEEN CONVENTIONAL INTEGRAL EQUATION AND NEW INTEGRAL EQUATION (27).

	Conventional Integral Equation	New Integral Equation (27)
Unknown function	$E(x)$	$E^C(x)$
Kernel function	$G(x\|x')$	$P(x\|x')$
Impressed term	incident wave	$F'(x)$
Integral region	$C = C_1 + C_2 + C_3 + C_4 C_5 + C_6$	$C = C_1 + C_2 + C_3 + C_4 + C_5 + C_6$

IV. Two-Mode Condition

So far, we have considered the case where the waveguides satisfy the single-mode condition. Let's next consider the case of multi-mode conditions. Since the general multi-mode conditions requires a complicated treatment, for simplicity, we explain the case where both waveguides satisfy the two-mode condition. Results for general multi-mode cases will be easily anticipated from this example. We assume that TE_{10} mode, denoted by $E_1^{-(2)}(x)$, is incident to the connection section from the waveguide 2. We assume that the total field should be given by the following expressions:

$$E(x) = E^C(x) + S_{21,1}E_1^{+(1)}(x) + S_{21,2}E_2^{+(1)}(x), \quad \text{in the waveguide 1,} \tag{28}$$

$$E(x) = E^C(x) + S_{22,1}E_1^{+(2)}(x) + S_{22,2}E_2^{+(2)}(x) + E_1^{-(2)}(x), \quad \text{in the waveguide 2,} \tag{29}$$

$$E(x) = E^C(x) \quad \text{in the connection section,} \tag{30}$$

where $S_{2j,i}$ $(i, j, = 1, 2)$ represent the scattering coefficients of TE_{i0} mode in the waveguide j for the case of incident from waveguide 2 and $E_i^{\pm(j)}(x)$ $(i, j = 1, 2)$ represents the mode function TE_{i0} mode in the waveguide j. Substituting (28), (29), and (30) into (1) and using Green's theorem (7) and (9), we can obtain the following relations in a way similar to that which has been used in the case of the single-mode condition:

$$E^C(x) + S_{21,1}U_1^{+(1)}(x) + S_{21,2}U_2^{+(1)}(x) = \int_C G(x|x')\,\partial E^C(x')/\partial n'\,dl' - S_{22,1}U_1^{+(2)}(x) - S_{22,2}U_2^{+(2)}(x) - U_1^{-(2)}(x) \tag{31}$$

where

$$U_i^{\pm(j)}(x) = \int_{C_{j0}} [G(x|x')\,\partial E_i^{\pm(j)}(x')/\partial n_j' - E_i^{\pm(j)}(x') \cdot \partial G(x|x')/\partial n_j']\,dl' \quad (i, j = 1, 2). \tag{32}$$

Substituting asymptotic expression (12) into (31) and following the procedure used in the previous section, we can obtain the following relations:

$$S_{21,1}M_1^{+(1)}(\theta_1) + S_{21,2}M_2^{+(1)}(\theta_1) + S_{22,1}M_1^{+(2)}(\theta_1) + S_{22,2}M_2^{+(2)}(\theta_1) = \int_C g(\theta_1|x')\,\partial E^C(x')/\partial n'\,dl' - M_1^{-(2)}(\theta_1) \tag{33}$$

$$S_{21,1}M_1^{+(1)}(\theta_2) + S_{21,2}M_2^{+(1)}(\theta_2) + S_{22,1}M_1^{+(2)}(\theta_2) + S_{22,2}M_2^{+(2)}(\theta_2) = \int_C g(\theta_2|x')\,\partial E^C(x')/\partial n'\,dl' - M_1^{-(2)}(\theta_2) \tag{34}$$

where

$$M_i^{\pm(j)}(\theta) = \int_{C_{j0}} [\,g(\theta|x')\,\partial E_i^{\pm(j)}(x')/\partial n_j' - E_i^{\pm(j)}(x')\,\partial g(\theta|x')/\partial n_j'\,]\,dl' \quad (i, j = 1, 2). \tag{35}$$

Since four unknown coefficients $S_{21,1}$, $S_{21,2}$, $S_{22,1}$ and $S_{22,2}$ exist in this case, they cannot be obtained from two relations (33) and (34). It is necessary to derive two more relations in order to determine these coefficients. They are obtained as follows: Substituting asymptotic expression (12) into (31), divide both sides of the resulting equation by the common function $A(r)$ and differentiate both sides of the resulting equation with respect to the variable angle θ. If we set $\theta = \theta_1$, $\theta = \theta_2$ and $r \to \infty$ in the final equation, we can obtain the following two relations as

$$S_{21,1}N_1^{+(1)}(\theta_1) + S_{21,2}N_2^{+(1)}(\theta_1) + S_{22,1}N_1^{+(2)}(\theta_1) + S_{22,2}N_2^{+(2)}(\theta_1) = \int_C h(\theta_1|x')\,\partial E^C(x')/\partial n'\,dl' - N_1^{-(2)}(\theta_1) \tag{36}$$

$$S_{21,1}N_1^{+(1)}(\theta_2) + S_{21,1}N_2^{+(1)}(\theta_2) + S_{22,1}N_1^{+(2)}(\theta_2) + S_{22,2}N_2^{+(2)}(\theta_2) = \int_C h(\theta_2|x')\,\partial E^C(x')/\partial n'\,dl' - N_1^{-(2)}(\theta_2) \tag{37}$$

where

$$N_i^{\pm(j)}(\theta) = \int_{C_{j0}} [h(\theta|x')\,\partial E_i^{\pm(j)}(x')/\partial n_j' - E_i^{\pm(j)}(x')\,\partial h(\theta|x')/\partial n_j']\,dl' \quad (i, j = 1, 2) \tag{38}$$

$$h(\theta|x') = \partial g(\theta|x')/\partial\theta = (-jn_rk_0x'\sin\theta + jk_0n_ry'\cos\theta) \cdot \exp(jn_rk_0x'\cos\theta + jk_0n_ry'\sin\theta). \tag{39}$$

The four unknown scattering coefficients can be determined from four independent relations (33), (34), (36) and (37) as

$$S_{21,1} = \left[\int W_1(x')\, \partial E^C(x')/\partial n'\, dl' + \Delta_{11} M_1^{-(2)}(\theta_1) + \Delta_{21} M_1^{-(2)}(\theta_2) + \Delta_{31} N_1^{-(2)}(\theta_1) + \Delta_{41} N_1^{-(2)}(\theta_1) \right] \Big/ \Xi \quad (40)$$

$$S_{21,2} = \left[\int W_2(x')\, \partial E^C(x')/\partial n'\, dl' + \Delta_{12} M_1^{-(2)}(\theta_1) + \Delta_{22} M_1^{-(2)}(\theta_2) + \Delta_{32} N_1^{-(2)}(\theta_1) + \Delta_{42} N_1^{-(2)}(\theta_1) \right] \Big/ \Xi \quad (41)$$

$$S_{22,1} = \left[\int V_1(x')\, \partial E^C(x')/\partial n'\, dl' + \Delta_{13} M_1^{-(2)}(\theta_1) + \Delta_{23} M_1^{-(2)}(\theta_2) + \Delta_{33} N_1^{-(2)}(\theta_1) + \Delta_{43} N_1^{-(2)}(\theta_1) \right] \Big/ \Xi \quad (42)$$

$$S_{22,2} = \left[\int V_2(x')\, \partial E^C(x')/\partial n'\, dl' + \Delta_{14} M_1^{-(2)}(\theta_1) + \Delta_{24} M_1^{-(2)}(\theta_2) + \Delta_{34} N_1^{-(2)}(\theta_1) + \Delta_{44} N_1^{-(2)}(\theta_1) \right] \Big/ \Xi \quad (43)$$

where

$$\begin{aligned} W_1(x') &= \Delta_{11} g(\theta_1|x') + \Delta_{21} g(\theta_2|x') + \Delta_{31} h(\theta_1|x') + \Delta_{41} h(\theta_2|x') \\ W_2(x') &= \Delta_{12} g(\theta_1|x') + \Delta_{22} g(\theta_2|x') + \Delta_{32} h(\theta_1|x') + \Delta_{42} h(\theta_2|x') \\ V_1(x') &= \Delta_{13} g(\theta_1|x') + \Delta_{23} g(\theta_2|x') + \Delta_{33} h(\theta_1|x') + \Delta_{43} h(\theta_2|x') \\ V_2(x') &= \Delta_{14} g(\theta_1|x') + \Delta_{24} g(\theta_2|x') + \Delta_{34} h(\theta_1|x') + \Delta_{44} h(\theta_2|x'), \end{aligned} \quad (44)$$

Ξ is the determinant of the matrix Q which is given by

$$Q = \begin{pmatrix} M_1^{+(1)}(\theta_1) & M_2^{+(1)}(\theta_1) & M_1^{+(2)}(\theta_1) & M_2^{+(2)}(\theta_1) \\ M_1^{+(1)}(\theta_2) & M_2^{+(1)}(\theta_2) & M_1^{+(2)}(\theta_2) & M_2^{+(2)}(\theta_2) \\ N_1^{+(1)}(\theta_1) & N_2^{+(1)}(\theta_1) & N_1^{+(2)}(\theta_1) & N_2^{+(2)}(\theta_1) \\ N_1^{+(1)}(\theta_2) & N_2^{+(1)}(\theta_2) & N_1^{+(2)}(\theta_2) & N_2^{+(2)}(\theta_2) \end{pmatrix} \quad (45)$$

and Δ_{ij} $(i, j = 1, 2, 3, 4)$ denotes the determinant of (i, j)-cofactor of matrix Q. Since the unknown coefficients are expressed in terms of the fields $\partial E^C(x')/\partial n$, we can also obtain a boundary integral equation for the case of two-mode condition formally identical to (27), where the kernel function $P(x|x')$ and the impressed term $F^i(x)$ are given by

$$P(x|x') = G(x|x') - [U_1^{+(1)}(x) W_1(x') + U_2^{+(1)}(x) W_2(x')]/\Xi - [U_1^{+(2)}(x) V_1(x') + U_2^{+(2)}(x) V_2(x')]/\Xi \quad (46)$$

and

$$\begin{aligned} F^i(x) = &-U_1^{-(2)}(x) \\ &- U_1^{+(1)}(x)[\Delta_{11} M_1^{-(2)}(\theta_1) + \Delta_{12} M_1^{-(2)}(\theta_2) + \Delta_{13} N_1^{-(2)}(\theta_1) + \Delta_{14} N_1^{-(2)}(\theta_2)]/\Xi \\ &- U_2^{+(1)}(x)[\Delta_{21} M_1^{-(2)}(\theta_1) + \Delta_{22} M_1^{-(2)}(\theta_2) + \Delta_{23} N_1^{-(2)}(\theta_1) + \Delta_{24} N_1^{-(2)}(\theta_2)]/\Xi \\ &- U_1^{+(2)}(x)[\Delta_{31} M_1^{-(2)}(\theta_1) + \Delta_{32} M_1^{-(2)}(\theta_2) + \Delta_{33} N_1^{-(2)}(\theta_1) + \Delta_{34} N_1^{-(2)}(\theta_2)]/\Xi \\ &- U_2^{+(2)}(x)[\Delta_{41} M_1^{-(2)}(\theta_1) + \Delta_{42} M_1^{-(2)}(\theta_2) + \Delta_{43} N_1^{-(2)}(\theta_1) + \Delta_{44} N_1^{-(2)}(\theta_2)]/\Xi, \end{aligned} \quad (47)$$

respectively.

V. Numerical Examples

In order to verify the validity of the integral equations, we use them for the numerical analysis of waveguide corner-bend. The integral equation (27) can be solved by the conventional boundary-element method (or moment-method). The basis functions used in the calculation in this paper are pulse functions and the testing functions are delta functions (point-matching). We first solved two types of right-angle waveguide corner-bend as shown in Fig. 2(a) and (b) which satisfy the single-mode condition. Table II shows numerical values of power transmission coefficient $|S_{21}|^2$ and power reflection coefficient $|S_{22}|^2$ and their total Total $= |S_{21}|^2 + |S_{22}|^2$ of the corner-bend of type(A) of Fig. 2(a) with varying the width of both waveguides from $2k_0a_1 = 2k_0a_2 = 1.10\pi$ to 1.90π. Table III shows the numerical values found in the case of the corner-bend of type(b) of Fig. 2(b). In these calculations, the waveguide 1 is truncate by the line $\beta_1\beta_1'$ and waveguide 2 is truncate by the line $\beta_2\beta_2'$ as shown in Fig. 2(a) and (b). Virtual boundary C_{10} is placed on the line $\alpha_1\alpha_1'$ which is perpendicular to C_1 and C_2, and C_{20} is placed on the line $\alpha_2\alpha_2'$ which is perpendicular to C_3 and C_4 as shown in Fig. 2(a) and (b). The parameters used in the calculations are $n_r = 1.0$, $k_0\overline{O\alpha_1} = k_0\overline{O\alpha_2} = 0.65$ (O is the corner point on the boundary C_5), and $k_0\overline{\alpha_1\beta_1} = k_0\overline{\alpha_1'\beta_1'} = k_0\overline{\alpha_2\beta_2} = k_0\overline{\alpha_2'\beta_2'} = 20.0$. The width of the basis pulse function normalized by wavenumber k_0 was 0.1 on the boundaries C_1–C_4 and it was adjusted to be about 0.1 on the boundaries C_5 and C_6 so that total number of un-

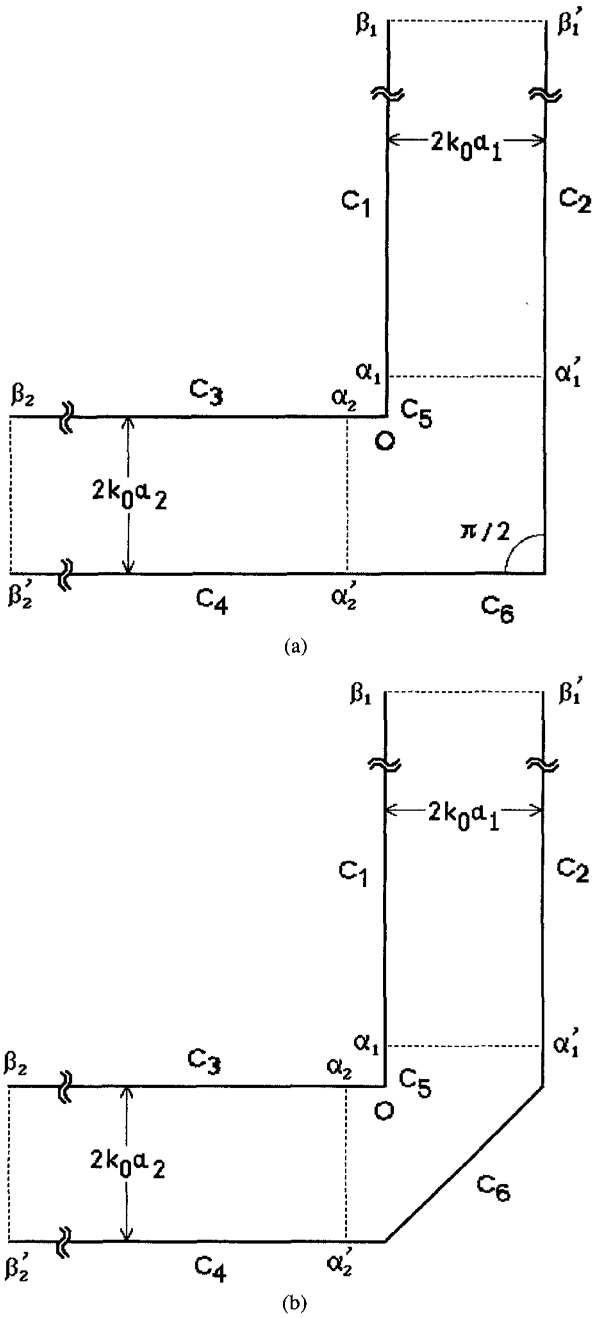

Fig. 2. (a) Waveguide right angle corner-bend of type (A). (b) Waveguide right angle corner-bend of type (B).

TABLE II
NUMERICAL VALUES OF POWER TRANSMISSION COEFFICIENT $|S_{21}|^2$, POWER REFLECTION COEFFICIENT $|S_{22}|^2$ AND THEIR TOTAL OF THE WAVEGUIDE BEND OF TYPE (A) UNDER THE SINGLE-MODE CONDITION

$2k_0 a_1$	$\|S_{21}\|^2$	$\|S_{22}\|^2$	Total
1.10 π	0.7236	0.2763	0.9999
1.20 π	0.8262	0.1737	0.9999
1.30 π	0.8570	0.1429	0.9999
1.40 π	0.8572	0.1427	0.9999
1.50 π	0.8272	0.1726	0.9998
1.60 π	0.7428	0.2571	0.9999
1.70 π	0.5376	0.4622	0.9998
1.80 π	0.1655	0.8345	1.0000
1.90 π	0.0156	0.9845	1.0001

TABLE III
NUMERICAL VALUES OF POWER TRANSMISSION COEFFICIENT $|S_{21}|^2$, POWER REFLECTION COEFFICIENT $|S_{22}|^2$ AND THEIR TOTAL OF THE WAVEGUIDE BEND OF TYPE (B) UNDER THE SINGLE-MODE CONDITION

$2k_0 a_1$	$\|S_{21}\|^2$	$\|S_{22}\|^2$	Total
1.10 π	0.2700	0.7299	0.9999
1.20 π	0.4686	0.5312	0.9998
1.30 π	0.6173	0.3826	0.9999
1.40 π	0.7299	0.2702	1.0001
1.50 π	0.8154	0.1846	1.0000
1.60 π	0.8803	0.1196	0.9999
1.70 π	0.9291	0.0706	0.9997
1.80 π	0.9646	0.0345	0.9991
1.90 π	0.9864	0.0093	0.9957

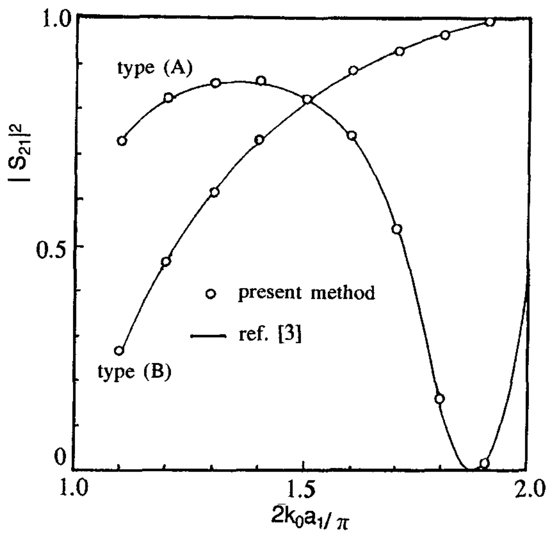

Fig. 3. Comparison of numerical results with those of [3].

knowns becomes 900. The comparison of these numerical results with the previous results are shown in Fig. 3 [3]. We can find that these results satisfy the power conservation and also agree with previous results very well. The virtual boundaries C_{10} and C_{20} can be placed at arbitrary positions in the uniform waveguides 1 and 2. In order to study the dependence of the results on the position of virtual boundaries, we changed positions of virtual boundary C_{10} for $\alpha_1 \alpha_1'$ to $\beta_1 \beta_1'$ parallel to the line $\alpha_1 \alpha_1'$ in the waveguide 1. Simultaneously, we changed the position of the boundary C_{20} from $\alpha_2 \alpha_2'$ to $\beta_2 \beta_2'$, parallel to the line $\alpha_2 \alpha_2'$ in the waveguides 2 as shown in Fig. 2(a). It is found that the numerical results are independent of the position of the boundaries C_{10} and C_{20}. It must be noted that when the virtual boundaries C_{10} and C_{20} are placed on lines $\beta_1 \beta_1'$ and $\beta_2 \beta_2'$, respectively, boundaries C_1, C_2, C_3, C_4 vanish and the boundary integral equation (27) for the field $E^C(x)$ becomes the integral equation only for the total field $E(x)$ having finite sized boundary of $C_5 + C_6$ as

$$0 = \int_{C_5 + C_6} P(x|x') \, \partial E(x') / \partial n' \, dl' + F^i(x) \quad (48)$$

by considering the notation (5). It is surprising that the waveguide discontinuity problems can be treated in the exactly same way without using mode-expansion tech-

TABLE IV

NUMERICAL VALUES OF POWER TRANSMISSION COEFFICIENT $|S_{21,1}|^2$ AND $\gamma_1|S_{21,2}|^2$, POWER REFLECTION COEFFICIENT $|S_{22,1}|^2$ AND $\gamma_1|S_{22,1}|^2$ AND THEIR TOTAL OF THE WAVEGUIDE BEND OF TYPE (A) UNDER THE TWO-MODE CONDITION (THE INCIDENT WAVE IS TE_{10} MODE AND γ_1 MEANS ENERGY SCALE FACTOR OF INCIDENT TE_{10} MODE)

$2k_0a_1$	$\|S_{21,1}\|^2$	$\|S_{22,1}\|^2$	$\gamma_1\|S_{21,2}\|^2$	$\gamma_1\|S_{22,2}\|^2$	Total
2.10 π	0.144	0.152	0.577	0.127	1.000
2.20 π	0.076	0.209	0.586	0.128	1.000
2.30 π	0.056	0.316	0.495	0.133	1.000
2.40 π	0.054	0.463	0.350	0.133	1.000
2.50 π	0.048	0.623	0.206	0.123	1.000
2.60 π	0.030	0.747	0.119	0.104	1.000
2.70 π	0.012	0.827	0.080	0.081	1.000
2.80 π	0.005	0.872	0.062	0.061	1.000
2.90 π	0.026	0.872	0.044	0.058	1.000

TABLE V

NUMERICAL VALUES OF POWER TRANSMISSION COEFFICIENT $\gamma_2|S_{22,1}|^2$ AND $|S_{21,2}|^2$, POWER REFLECTION COEFFICIENT $\gamma_2|S_{22,1}|^2$ AND $|S_{22,1}|^2$ AND THEIR TOTAL OF THE WAVEGUIDE BEND OF TYPE (A) UNDER THE TWO-MODE CONDITION (THE INCIDENT WAVE IS TE_{20} MODE AND γ_2 MEANS ENERGY SCALE FACTOR OF INCIDENT TE_{20} MODE)

$2k_0a_1$	$\gamma_2\|S_{21,1}\|^2$	$\gamma_2\|S_{22,1}\|^2$	$\|S_{21,2}\|^2$	$\|S_{22,2}\|^2$	Total
2.10 π	0.577	0.127	0.143	0.153	1.000
2.20 π	0.586	0.128	0.221	0.065	1.000
2.30 π	0.495	0.133	0.346	0.026	1.000
2.40 π	0.350	0.133	0.506	0.011	1.000
2.50 π	0.206	0.123	0.662	0.008	0.999
2.60 π	0.119	0.104	0.765	0.012	1.000
2.70 π	0.080	0.081	0.821	0.018	1.000
2.80 π	0.062	0.061	0.853	0.023	0.999
2.90 π	0.044	0.058	0.860	0.037	0.999

niques as that for the scattering problems by the isolated finite-sized metallic objects whose shape is given by Fig. 2(a) and (b).

For the case where the two-mode condition is satisfied, numerical values of power transmission coefficients $|S_{21,1}|^2$, $\gamma_1 \cdot |S_{21,2}|^2$ and power reflection coefficients $|S_{22,1}|^2$, $\gamma_1 \cdot |S_{22,2}|^2$, and their total Total $= |S_{21,1}|^2 + \gamma_1 \cdot |S_{21,2}|^2 + |S_{22,1}|^2 + \gamma_1 \cdot |S_{22,2}|^2$ of the corner-bend of type(A) of Fig. 2(a) are shown in Table IV with varying the width of the both waveguides from $2k_0a_1 = 2k_0a_2 = 2.10\pi$ to 2.90π for the case of incident TE_{10} mode. The results for the incident TE_{20} mode are shown in Table V. In these Tables, constants γ_1 and γ_2 mean energy scale factor of incident TE_{10} and TE_{20} mode, respectively, which are defined by

$$\begin{pmatrix}\gamma_1\\ \gamma_2\end{pmatrix} = (\text{energy of } {}^{TE_{20}}_{TE_{10}} \text{ mode of unit amplitude}) / (\text{energy of } {}^{TE_{10}}_{TE_{20}} \text{ mode of unit amplitude}).$$

These results also satisfy the energy conservation and reciprocity ($\gamma_k|S_{2i,j}|^2$ of incident TE_{k0} mode) $=$ ($\gamma_j|S_{2i,k}|^2$ of incident TE_{j0} mode) ($i, j, k = 1, 2$) and show the validity of the integral equation (27) for the problems which satisfy the two-mode condition.

VI. CONCLUSION

The novel integral equations which can be called guided-mode extracted integral equations (GMEIE's) for the basic theory of CAD software of various waveguide circuits has been presented. As rather simple examples, concrete expressions of new boundary integral equations for the corner-bend of metallic waveguides which satisfy the single-mode and two-mode conditions have been obtained. By using the integral equations, we can treat the waveguide discontinuity problem like the scattering problem of isolated finite-sized metallic objects. The basic idea of the new integral equation is very general. Hence, the GMEIE is applicable to the more complicated waveguide circuits having more than two ports or the dielectric open waveguide circuits [8]–[10]. Since the GMEIE does not employ the mode expansion techniques, it will be easily applicable to three dimensional problems. The theory used in the GMEIE is also applicable to problems of other fields such as acoustic, elastic waves.

ACKNOWLEDGMENT

We thank Mr. O. Ogami, Mr. H. Ootera and Mr. Y. Hosoe of Gifu University for their help in preparation of this paper.

REFERENCES

[1] E. Tonye and H. Baudrand, "Multimode s-parameter of planar multiport junctions by boundary element method," *Electron. Lett.*, vol. 20, pp. 799–802, Sept. 1984.

[2] H. Sano and S. Kurazono, "An analysis of Michelson interferometer-type hybrid to boundary element method," *Trans. Inst. Electron. Commun. Eng. Japan*, vol. J67-B, pp. 1392–1398, Dec. 1984.

[3] M. Koshiba and M. Suzuki, "Application of the boundary element method to waveguide discontinuities," *IEEE Trans. Microwave Theory Tech.*, vol. MTT-34, pp. 301–307, Feb. 1986.

[4] S. Kagami and I. Fukai, "Application of boundary-element method to electromagnetic field problems," *IEEE Trans. Microwave Theory Tech.*, vol. MTT-32, pp. 455–461, Apr. 1984.

[5] K. Ise and M. Koshiba, "Numerical analysis of H-plane waveguide junctions with dielectric post by combination of finite and boundary elements," *Trans. Inst. Electron. Commun. Eng. Japan*, vol. J71-C, pp. 250–258, Feb. 1988.

[6] K. Ise and M. Koshiba, "Numerical analysis of H-plane waveguide junctions by combination of finite and boundary elements," *IEEE Trans. Microwave Theory Tech.*, vol. 36, pp. 1343–1351, Sept. 1988.

[7] K. Tanaka and M. Kojima, "New boundary integral equation for CAD of waveguide circuit," *Electron. Lett.*, vol. 24, no. 13, pp. 807–808, June 1988.

[8] K. Tanaka and M. Kojima, "New boundary integral equations for computer-aided design of dielectric waveguide circuits," *J. Opt. Soc. Am. A*, vol. 6, pp. 667–674, May 1989.

[9] K. Tanaka, "New boundary integral equations for CAD of dielectric optical circuits," in *Proc. ISAP'89*, Aug. 1989, pp. 145–149.

[10] —–, "New boundary integral equations for CAD of dielectric waveguide discontinuities," in *1991 AP-S Symp. Dig.*, vol. 2, June 1991, pp. 870–873.

Kazuo Tanaka (M'75) was born in Mie Prefecture, Japan on June 7, 1947. He received the B.E., M.E., and Ph.D., degrees in electrical communication engineering from Osaka University, Osaka, Japan, in 1970, 1972, and 1975, respectively.

In 1975, he became a Research Associate in the Department of Electrical Engineering at Gifu University. He was appointed Associate Professor in the Department of Electronics and Computer Engineering there in 1985 and in 1990 he was named

Professor. His research work since 1970 has been on a general-relativistic electromagnetic theory and application, computational electromagnetic, and radiographic image processing and he is currently interested in the CAD of integrated optical circuits.

Dr. Tanaka is a member of the Institute of Electronics, Information and Communication Engineers of Japan, the Physical Society of Japan, the Information Processing Society of Japan and the Japan Society of Medical Imaging and Information Science (MII). In 1987, he was awarded the Uchida Paper Award by the MII.

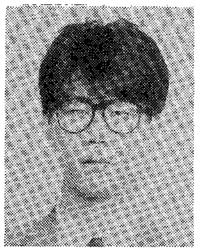

Masaaki Nakahara was born in Gifu Prefecture, Japan on February 9, 1967. He received the B.S. and M.S. degrees in electrical engineering from Gifu University, Gifu, Japan, in 1989 and 1991, respectively.

Since 1991 he has been employed by the Japan IBM Corporation, Tokyo, Japan.

Mr. Nakahara is a member of the Institute of Electronics and Communication Engineers of Japan.